

Concrete spalling: Interaction between tensile behaviour and pore pressure during heating

Roberto Felicetti and Francesco Lo Monte

Politecnico di Milano, Milan, Italy

Abstract. Explosive spalling is generally considered to be caused by concrete fracturing due to the interaction of (a) the pore pressure induced by moisture transport and vaporization and (b) the stress induced by thermal gradients and external loads. In order to investigate the first point, a special setup has been designed and an experimental campaign has been recently launched at the Politecnico di Milano, regarding ten different concrete mixes, characterized by different compressive strength, aggregate and fiber types.

1. INTRODUCTION

Explosive concrete spalling is generally considered to be caused by the interaction of (a) the pore pressure induced by vaporization and moisture transport and (b) the stress induced by thermal gradients and external loads [1, 2]. Despite of a number of studies on this topic [3, 4], stressing the role of both internal material factors (moisture content, porosity, tensile strength, fiber content) and external structural factors (heating rate, applied loads and constraints), how these different aspects influence each other is not completely clear.

Considering concrete as a multi-phase porous media, the total stress σ^{tot} can be split into the effective stress σ^{eff} , borne by the solid skeleton, and the solid phase pressure p^s exerted by the pore fluids [5]: $\sigma^{\text{tot}} = \sigma^{\text{eff}} - p^s \cdot \mathbf{I}$, where \mathbf{I} is the unit tensor (tensile stress and pressure are assumed positive). The critical issue is to understand how solid pressure p^s is related to the pressure of the different fluids (liquid water, gas = vapour + dry air). In Table 1 some expressions suggested in the literature are reported. One general remark is that exceeding the “tensile strength” is the macroscopic result of an unstable flaw propagation through the porous network where fluid pressure is exerted. Considering the influence of pressure in this internal instability would be a more consistent way to understand the role played by water (liquid and vapour) in triggering spalling.

Within this context two experimental campaigns have been planned at the Politecnico di Milano, based on a special setup aimed at performing simple indirect-tension tests (split-cube tests) under different levels of sustained pore pressure [6]. The tests are performed on cubic specimens, which are heated on two opposite faces and sealed/insulated on the remaining four sides (see Fig. 1a), so to induce quasi mono-dimensional thermal and hygral fluxes. During heating, both temperature and pressure are monitored in the centroid of the specimen and when pore pressure reaches the peak value, the splitting test is performed, involving a fracture on the symmetry plane (Fig. 1a).

The *first experimental campaign* involved the concrete type B40, thoroughly investigated in [7], a Normal Strength Concrete for which spalling is unlikely to occur. Two batches were cast: with and without monofilament polypropylene fiber (2 kg/m^3 ; $\phi = 18 \mu\text{m}$ and $L = 12 \text{ mm}$). This first test series allowed to ascertain the role of fiber content and heating rate on the peak values of pore pressure and the consequent decrease of the apparent tensile strength.

This is an Open Access article distributed under the terms of the Creative Commons Attribution License 2.0, which permits unrestricted use, distribution, and reproduction in any medium, provided the original work is properly cited.

Table 1. Solid-fluid pressure relation according to different authors. p^{gas} , p^c = gas, capillary pressure.

$p^s = p^{\text{gas}} - \chi p^c$	Gawin et al., 2011 [9]
$p^s = p^{\text{gas}}$	Tenchez and Purnell, 2005 [10]
$p^s = \text{porosity } p^{\text{gas}}$	Dwaikat and Kodur, 2009 [2]
$p^s \approx 0.8 p^{\text{gas}}$	Ichikawa and England, 2004 [11]

The *second experimental campaign*, recently launched at the Politecnico di Milano, is focused on the influence of concrete grade and mix design (see [8]):

- three concrete grades, $f_{\text{cube}} \geq 45, 70, 95$ MPa (named M45, M70 and M95, respectively);
- for the intermediate grade, different aggregate types are considered (silico-calcareous, calcareous and basalt aggregates; silico-calcareous aggregate is considered as reference);
- for the intermediate grade with silico-calcareous aggregate, both plain concrete and fiber concrete are considered; different kind of fibers are added to the mix, namely steel fiber (in order to investigate the role played by the increased ductility of concrete in the post-peak behavior), and polypropylene fiber (both monofilament and fibrillated).

Besides confirming the first results, this latter investigation aims at linking the macroscopic mechanical effects to the concrete microstructure (porosity, permeability, chemo-physical transformations) as a tentative to validate the pore pressure as a leading factor governing spalling. So far, only silico-calcareous plain concretes have been investigated.

2. EXPERIMENTAL PROGRAM

The starting idea of the test setup is to instate the monodimensional hygro-thermal problem of a thin wall heated on both sides. The thermal gradients lead to the formation of thermal stress (compression in the hot layers and tensile stress in the core), while the vaporization of water causes a significant increase of the pressure (from 1–2 MPa in Normal Strength Concrete to 4–5 MPa in High Performance Concrete).

Pore pressure and vaporization cause moisture transport according to the Darcy's law (due to pressure gradient and related to fluid permeability in the porous media) and to the Fick's law (due to concentration gradients and related to vapour diffusivity in dry air). Moisture (water and/or vapour) flows both towards the hottest and the inner layers. In this latter case, condensation may occur, leading to the possible formation of a quasi-saturated layer with reduced gas permeability [1].

The temperature field across the wall is governed by the well-known Fourier's law; being vaporization an endothermic process, the hygro-thermal problem is coupled. The compressive stress (parallel to the heated face) contributes to trigger spalling by decreasing the mechanical stability of the system.

2.1 Heating procedure

The heating system consisted of two radiant panels facing two opposite sides of the concrete sample (Figs. 1b), in order to guarantee the symmetrical heating with respect to the mid-plane of the specimen. Radiant panels allowed to obtain a variety of heating rates thanks to the built-in thermocouples connected to separate controllers. The choice of the heating rate is quite critical because very high heating rates cause severe damage (i.e. cracking) in the concrete due to thermal stress (hence, low values of pore pressure, the vapour being free to escape through the microcracks), while very low heating rates cause significant drying (leading, again, to low values of pore pressure). The effect of this parameter was investigated in the first experimental campaign on concrete B40; four different heating rates were applied: a slow rate (1 °C/min), two intermediate values (2 and 10 °C/min) and a fast rate (120 °C/min, equal to the mean heating rate in the first four minutes of Standard Fire). Once the external temperature

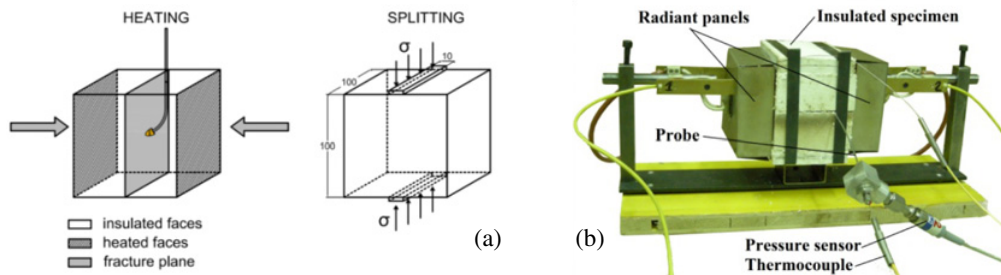


Figure 1. (a) Scheme of heating and splitting; and (b) specimen during heating.

reached 600 °C, it was kept constant. In the second experimental campaign 2 °C/min was used for Mix M45 and 0.5 °C/min for Mixes M70 and M95.

A critical issue is thermal insulation, necessary to create a mono-dimensional heat flux. Hence, the four unheated faces were covered with 20 mm-thick ceramic fiber boards (Fig. 1b).

Numerical analyses were performed to check the effectiveness of the insulation (Sect. 3.3). On the other hand, sealing is fundamental in creating a mono-dimensional hygral flux, by preventing the specimen from drying through the lateral faces. Different combinations of materials were tested and the best proved to be aluminium foils glued with temperature resistant epoxy [6]. Finally, the aluminium foils were cut along the splitting lines on two opposite faces, in order to prevent any contribution to the tensile strength of the cube; then the thin cuts were sealed with silicon.

2.2 Pore pressure measurements and splitting test

The measurement of the pore pressure was performed by using capillary stainless steel pipes fitted with sintered metal heads. Great attention was paid to the shape of both the head and the pipe, in order not to affect concrete mechanical response. Curved pipes (Fig. 1a) were used, in order to prevent the probes from lying in the mid-plane of the cube (that is the fracture plane in the splitting test). The pipes were filled with silicon oil and had a thermocouple inside. Hence, both pressure and temperature inside the head of the probe were measured.

Testing in tension was performed by splitting [12], which requires a rather simple test setup and can be easily implemented in the case of hot specimens; contrary to bending tests, this technique brings in far less structural effects, with an almost constant ratio between the indirect tensile strength and the “true” tensile strength [13]. In order to define the reference tensile strength in virgin condition, splitting tests were performed on unheated specimens (the results are shown in the inserts in Fig. 6). In the hot test, both pressure and temperature were monitored in the centroid of the specimen. When the maximum pore pressure was reached, the splitting test was performed, while continuously measuring pressure and temperature.

2.3 Mix design, casting and curing

Concrete B40 consists of calcareous aggregates ($d_a \leq 20$ mm), 437 kg/m³ of cement and water to cement ratio = 0.54 (see [6]). Mixes M45, M70 and M95 consist of silico-calcareous aggregate ($d_a \leq 16$ mm), 400 kg/m³ of cement for Mixes M45 and M75 and 480 kg/m³ for Mix M95, and water to cement ratio = 0.56, 0.36 and 0.24 for M45, M70 and M95, respectively (see [8]).

Specimens were cast in 10 cm-side plastic cubic moulds and were de-moulded after one day. Then they were sealed in bags for one week. Afterwards, the bags were opened and the cubes were kept in laboratory environment for three weeks. Finally, the bags were closed in order to prevent drying due to air exposure, until experiments were conducted (more than 60 days after casting).

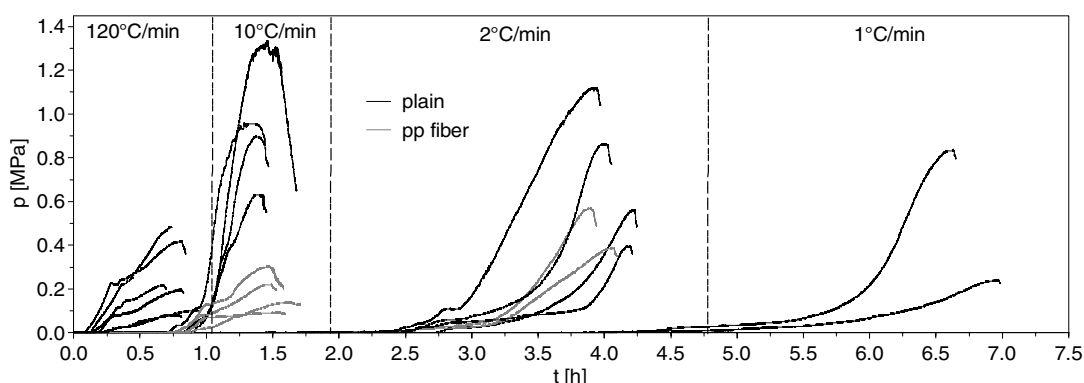


Figure 2. Pressure development in the centroid as a function of time.

3. TEST RESULTS ON CONCRETE B40

3.1 Pore pressure development during heating

In Fig. 2, the experimental results on concrete B40 for the four heating are shown in terms of pressure-time curves. The results confirm the pore pressure values obtained in [7].

The experimental results showed that:

- the qualitative development of pore pressure is similar for all the tests: the dramatic pressure rise occurs almost at the beginning of a temperature plateau (= start of water vaporization) and the peak is achieved at the end of this plateau;
- the irregular shape of the pressure-time curves for HR = 120 °C/min indicates concrete cracking, probably due to the thermal stress (this is substantiated by the numerical results, see Sect. 3.3);
- intermediate heating rates (2 and 10 °C/min) cause pore pressure plots to lie close to the saturation vapour pressure curve, whereas significant gaps are observed for slow and high heating rates (1 and 120 °C/min), probably due to a more pronounced drying and cracking, respectively (in fact, lower values of pore pressure were obtained, see Fig. 2);
- in fiber concrete, pore pressure is even more than 75% lower than in plain concrete.

The dispersion of the pressure peaks at the same nominal testing conditions can be ascribed to some variability among specimens in the effectiveness of the sealing system or in the moisture content. Nonetheless, this is functional for performing the fracture test under the same thermo-mechanical conditions but different pressures.

3.2 Pore pressure and indirect tensile strength

As mentioned before, splitting tests were performed when maximum pore pressure was reached; this means that experiments had not been performed at a specific temperature. However, peak pressures were achieved in a narrow range of temperature (175 °C to 225 °C). Then, the possible chemo-physical decay of concrete may be assumed uniform in the whole set of specimens. The results obtained from the splitting tests are reported in Fig. 3 as a function of the pressure measured during the test. A linear regression has been performed, obtaining a negative slope $k = -1.24$ independently on both the heating rate and fiber content.

Hence, it can be inferred that the detrimental effect of pore pressure on the indirect tensile strength is almost independent on the heating rate and it revealed to be linear and proportional to a value greater than one. On the other hand, the intercept of the lines strongly depends on the heating rate (Table 2). This is the combined effect of the possible internal deterioration due to heating and the influence of

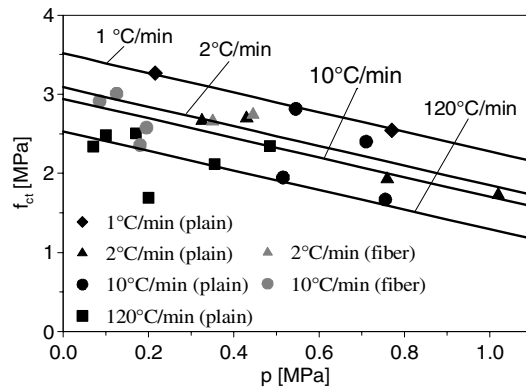


Figure 3. Tensile strength-pore pressure plot.

Table 2. Apparent tensile strength for null pore pressure evaluated according to the regression lines f_{ct}^{th} (intercepts of the four straight lines) and numerically (f_{ct}^{num}) for the different heating rates. $f_{ct}^{20} = 3.6$ MPa.

HR [° C/min]	f_{ct}^{th} [MPa]	f_{ct}^{th} /	f_{ct}^{num} f_{ct}^{20} [MPa]	$f_{ct}^{num}/$ f_{ct}^{20}
1	3.51	0.98	3.31	0.92
2	3.09	0.86	3.21	0.89
10	2.94	0.82	2.95	0.82
120	2.53	0.70	2.68	0.74

thermal stress induced by temperature gradients. At the slowest heating rate (1 °C/min) the intercept is 98% of the tensile strength in virgin cubes; this indicates that the material decay up to 220 – 230 °C is negligible.

Increasing the heating rate up to 120 °C/min, a sizeable reduction of the tensile strength at zero pressure becomes evident, leading to a decay of about 30%. These results are consistent with the thermal-induced damage, as shown by numerical analyses (see Sect. 3.3).

3.3 Numerical investigation on the effect of the heating rate

Thermo-mechanical numerical analyses were performed by means of ABAQUS FE code, by modelling one eighth of the insulated cube (Fig. 4a,b). The mechanical behaviour was simulated through Concrete Damaged Plasticity Model, implemented in ABAQUS.

The curves suggested by the EC2 [14] were used for the variation with the temperature of both concrete density and conductivity (the lower limit was adopted), while the specific heat was evaluated through back analysis of the experimental values of temperature measured in the centroid of the specimens. The curve suggested by EC2 was used for the decay of the compressive strength with the temperature (calcareous concrete); on the other hand, the decay of the tensile strength was modelled by extending the range in which tensile behaviour is constant (up to 230 °C) on the basis of the experimental results.

For concrete in compression, the EC2 stress-strain relation was adapted by adjusting the strain at the peak so to match the initial material stiffness. The initial stiffness was worked out on the basis of the load-induced strain observed in the loaded heating tests performed in [7]. The thermal strain was taken from the same set of results.

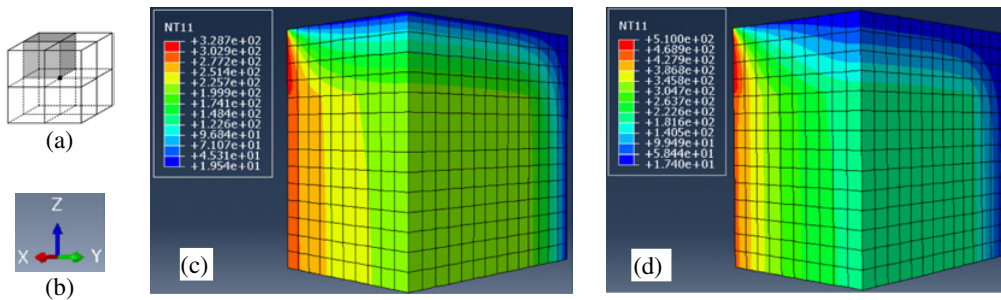


Figure 4. (a) Modelled eight of the specimen, (b) reference system – y, long. direction; distribution of the temperature just before splitting test for HR = 1 °C/min (c) and 120 °C/min (d).

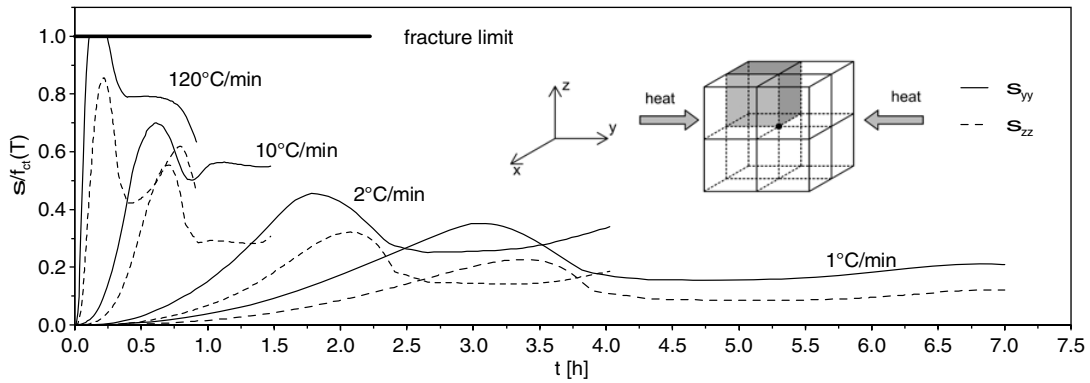


Figure 5. Thermal stress in the centroid of the specimen for the four heating rates according to the numerical analyses.

In tension, a bilinear model was considered; fracture energy G_f was evaluated according to [15] and kept constant with the temperature. Numerical analyses were performed to simulate both the heating and the following splitting test. The temperature distributions just before the splitting test (showed in Fig. 4c,d for HR = 1 and 120 °C/min, respectively) prove the effectiveness of the insulation layer in creating a mono-dimensional heat flux.

In Fig. 5 the tensile stress in the centroid of the specimen during heating is shown as a functions of time for all the investigated heating rates (1, 2, 10 and 120 °C/min). As expected, fast heating induces much higher thermal stress than slow heating. However, only the highest rate causes concrete cracking ($\sigma/f_{ct}(T) = 1$ in Fig. 5). This result is consistent with the irregular growth of the measured pore pressure during the experimental tests with HR = 120 °C/min. Moreover, thermal stress has an influence also on the peak load of the hot splitting test. In Table 2 the numerical values of splitting tensile strength for the different heating rates are reported together with the intercept of the four regression lines. The agreement between numerical and experimental results is satisfactory, showing a good reliability of the implemented thermo-mechanical model.

4. TEST RESULTS ON MIXES M45 AND M70

The same experimental procedure is being applied on other concrete mixes. So far, three mixes have been investigated (M45, M70 and M95) and the results are shown in Fig. 6a in terms of normalized

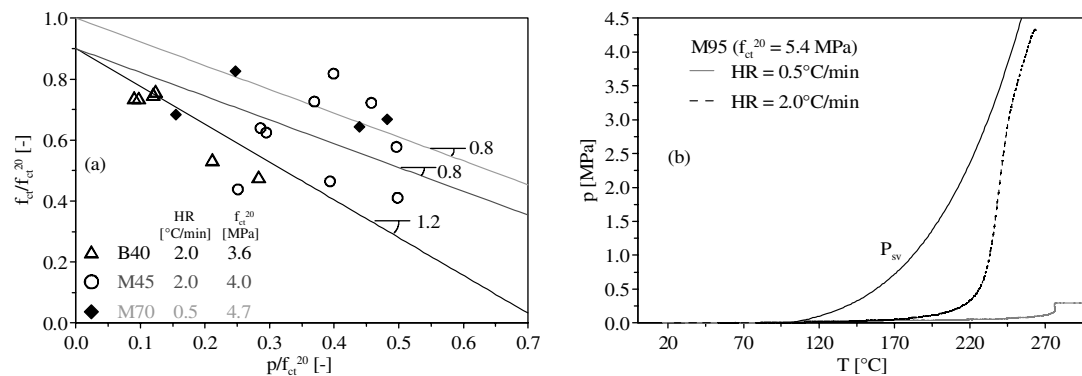


Figure 6. (a) Tensile strength-pore pressure plot for Mixes B40, M45 and M70; and (b) pore pressure development as a function of the temperature for two M95 specimens.

apparent tensile strength (f_{ct}/f_{ct}^{20}) as a function of the normalized pore pressure (p/f_{ct}^{20}). In Fig. 6a also the values corresponding to concrete B40 for $HR = 2^\circ\text{C}/\text{min}$ are reported. Mixes B40, M45 and M70 show a similar trend, indicating that pore pressure induces a decay in the apparent tensile strength by a quantity close to the pressure itself: the negative slope of the regression lines goes from -0.8 for M45 and M70 to -1.2 for B40.

This difference can be ascribed to the higher pressures measured in the case of Mixes M45 and M70 (up to 2.4 MPa) with respect to concrete B40 (less than 1.4 MPa). In fact, for high peak values it is difficult to have a uniform distribution of pressure in the fracture plane, becoming the sealing system less efficient; this means that the average pressure in the fracture plane is lower than the measured pressure. Hence the obtained slope has to be considered as a lower limit of the real one. However, it should be observed that the absolute values of the slope are definitively higher than the porosity ($\approx 10\%$ by volume), confirming that pore pressure causes a decrease of the apparent tensile strength of about the same order of magnitude of the pressure itself.

It is worth noticing that the heating rates for the mixes are different ($HR = 2^\circ\text{C}/\text{min}$ for B40 and M45 and $HR = 0.5^\circ\text{C}/\text{min}$ for M70 and M95). The use of a slower heating rate for M70 and M95 with respect to the other two mixes was required by problems arising to the pressure measuring system.

In some tests performed on M70 and M95, with $HR = 2^\circ\text{C}/\text{min}$, a very low pore pressure was measured in spite of the following violent explosion during the splitting tests (together with the expulsion of a considerable amount of vapour). This indicates that the measured pressure was definitely lower than the actual pressure inside the specimen. Such evidence reminds the surprising results reported in [16], in which plain concrete exhibited very low pressures and a remarkable spalling, whereas polypropylene fiber concrete showed higher pressures and no spalling at all. One possible explanation is that for very dense cementitious matrices, water saturation is reached around the sensor, so preventing the fluid to flow towards the probe (hence, no pressure is transmitted). Only choosing a very slow heating rate, which favours both drying and moisture transport, significant values of pore pressure were reached (see Fig. 6b). However, this phenomenon is still under investigation.

5. INTERPRETATION OF THE EXPERIMENTAL RESULTS

The apparent tensile strength measured in the experimental tests is a function of the real material strength (including only the effect of thermo-physical transformation occurring at the temperature T), the pore pressure developed in the pores and the detrimental effect of thermal stress due to the inhomogeneous

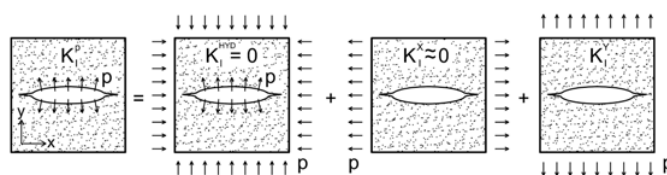


Figure 7. Square part of concrete with one defect.

heating. In the present work, both the real material strength decay (for the investigated temperatures) and the effect of the thermal stress in case of slow heating rate proved to be negligible. The effect of pore pressure seems to confirm the approach based on the effective stress assuming $p^s = p^{gas}$ for any porosity and neglecting the role of the capillary pressure [10]. One possible interpretation is based on fracture mechanics and on the stability of the inherent material defects.

The tensile behaviour of concrete may be interpreted as the global effect of many micro defects, which reach an unstable propagation when a critical level of stress is reached.

This means that pressure exerted inside defects (pores) is equivalent, from the fracture mechanics point of view, to an intensification of the tensile stress by the same value. This conclusion complies with the experimental results.

Let us consider a concrete element including a defect which governs the material tensile response on the y direction (Fig. 7). Pressure p, exerted inside the defect, can be equivalently considered as the sum of three loading cases: hydrostatic pressure in the whole body, external tensile stress on both x and y directions. Hydrostatic pressure has no effect on fracture propagation ($K_I^{HYD} = 0$); moreover, for sharp-shaped defects, the stress intensification due to parallel loading is negligible ($K_I^X \approx 0$) compared to the effect of transverse loading (K_I^Y).

6. CONCLUSIONS

In this paper the influence of transient thermo-hygral conditions on the fracture response of concrete was investigated. The main conclusions that can be drawn on the basis of a comprehensive experimental program are summarized in the following:

- for Normal Strength Concrete, intermediate heating rates (2 and 10 °C/min) allow to measure higher pore pressures, while fast heating rate (120 °C/min) causes severe thermal stress which sizeably affects the experimental results;
- pore pressure decreases the apparent tensile strength of concrete by a quantity of the same order of magnitude of the pressure itself (from 0.8 to 1.2 times the pressure), almost independently from both fiber content and heating rate.

Based on the above-discussed experimental campaigns, pore pressure seems to play a major role in triggering explosive spalling. As a partial confirmation, in the hot splitting tests the fracture process showed to be dramatically faster than in ordinary tests and the two halves of the split cube were violently projected apart. However, there is a not yet experimental proof that pore pressure can cause, by itself, spalling; complementary work should be carried out to study this possible mechanism in order to enlighten the influence of moisture clog, liquid water pressure and material stress.

The authors wish to thank Mehmet Baran Ulak and Murat Hacıoglu from Turkey, Davide Sciancalepore and Alessandro Simonini from Italy, and Jihad MD Miah and Shamima Aktar from Bangladesh, who actively contributed to this study in partial fulfilment of their MS degree requirements at Politecnico di Milano.

References

- [1] Kalifa P., Menneteau F. D., Quenard D., Spalling and pore pressure in HPC at high temperatures, *Cement and Concrete Research*, 30, 1915–1927, 2000
- [2] Dwaikat M.D. and Kodur V.K.R., Hydrothermal Model for Predicting Fire-induced Spalling in Concrete Structural Systems, *Fire Safety Journal*, 44, 425–34, 2009.
- [3] fib BULLETIN 38: Fire design of concrete structures - Materials, structures and modelling, International Federation for Structural Concrete (fib), Lausanne, 2007.
- [4] Khoury A. G., Effect of fire on concrete and concrete structures, *Progress in Structural Engineering and Materials*, 2, 429–447, 2000.
- [5] Gray W.G. and Schrefeer B.A., Analysis of the solid phase stress tensor in multiphase porous media, *Int. J. for Numerical and Analytical Methods in Geomechanics*, 31, 541–581, 2007.
- [6] Felicetti R., Lo Monte F., Pimienta P., The influence of pore pressure on the apparent tensile strength of concrete, Proceedings of the 7th International Conference on Structures in Fire, M. Fontana, A. Frangi, M. Knobloch (Eds.), Zurich, Switzerland, 6–8 June, 589–598, 2012.
- [7] Mindeguia J. C., Pimienta P., Carre H., La Borderie Ch., Experimental study on the contribution of pore vapour pressure to the thermal instability risk of concrete, 1st Int. Work. on Concrete Spalling due to Fire Exposure, Leipzig (Germany), 150–167, 3–5 Sept. 2009.
- [8] Rossino C., Lo Monte F., Cangiano S., Felicetti R. and Gambarova P.G., Concrete Spalling Sensitivity versus Microstructure: Preliminary Results on the Effect of Polypropylene Fibers, Proceedings of the 3th International Workshop on Concrete Spalling due to Fire Exposure, Paris, France, 25–27 September, 2013, in press.
- [9] Gawin D., Pesavento P and Schrefler B.A., What physical phenomena can be neglected when modelling concrete at high temperature? A comparative study. Part 1 and 2, *International Journal of Solids and Structures*, 48, 1927–1961, 2011.
- [10] Tenchev R., Purnell P., An application of a damage constitutive model to concrete at high temperature and prediction of spalling, *Int. J. of Solids and Structures*, 42, 6550–6565, 2005.
- [11] Ichikawa, Y., England, G.L., Prediction of moisture migration and pore pressure build-up in concrete at high temperatures, *Nuclear Engineering and Design*, 228, 245–259, 2004.
- [12] CEN European Committee For Standardization, EN 12390-6, Testing hardened concrete, Part 6: Tensile splitting strength of test specimens, European Standard, 2000.
- [13] Bamonte P. and Felicetti R., High-Temperature Behaviour of Concrete in Tension, *Structural Engineering International*, 4, 493–499, 2012.
- [14] EN 1992-1-2:2004, Eurocode 2 - Design of concrete structures - Part 1-2: General rules - Structural fire design, European Comm. for Standardization (CEN), Brussels (Belgium), 2004.
- [15] CEB – fib Model Code 1990, Comité Euro-Int. du Béton, Lausanne (Switzerland), 1993.
- [16] Jansson R. and Bostrom L., The Influence of Pressure in the Pore System on Fire Spalling of Concrete, *Fire Technology*, 46, 217–230, 2010.